Environ. Sci. Technol. **2006**, *40,* 6392−6397

Magnitude and Directional Measures of Water and Cr(VI) Fluxes by Passive Flux Meter

TIMOTHY J. CAMPBELL,[†] KIRK HATFIELD,*[,†] HARALD KLAMMLER,[†] MICHAEL D. ANNABLE,[‡] AND P. S. C. RAO[§]

Department of Civil & Coastal Engineering, University of Florida, P.O. Box 116580, Gainesville, Florida 32611-6580, Department of Environmental Engineering Science, University of Florida, 345 Weil Hall, Gainesville, Florida 32603, and School of Civil Engineering, Purdue University, 550 Stadium Mall Drive, West Lafayette, Indiana 47907-2051

A new configuration of the passive fluxmeter (PFM) is presented that provides for simultaneous measurements of both the magnitude and the direction of ambient groundwater specific discharge q_0 and Cr(VI) mass flux J_{Cr}. The PFM is configured as a cylindrical unit with an interior divided into a center section and three outer sectors, each packed with a granular anion exchange resin having high sorption capacity for the Cr(VI) oxyanions CrO_4^{2-} and $HCrO_4^-$. The sorbent in the center section is preloaded with benzoate as the "resident" tracer. Laboratory experiments were conducted in which PFMs were placed in porous packed bed columns, through which was passed a measured volume of synthetic groundwater containing Cr(VI). During the deployment period, some of the resident tracer is depleted while the Cr(VI) is sorbed. The resin was then removed from the four sectors separately and extracted to determine the "captured" mass of Cr(VI) and the residual mass of the resident tracer in each. Cumulative specific discharge, q_0t, values were assessed using the residual mass of benzoate retained in the center section. The direction of this discharge φ was ascertained from the mass distribution of benzoate intercepted and retained in the outer three sections of the PFM. Cumulative chromium fluxes, $J_{Cr}t$, were quantified using the total Cr(VI) mass intercepted and retained on the PFM. Experiments produced an average measurement error for direction φ of 3° ± 14°, while the average measurement errors for q_0 and J_{Cr} were, respectively, −8% ±15% and −12% ±23%. Results demonstrate the potential utility of the new PFM configuration for characterizing groundwater and contaminant fluxes.

Introduction

Chromium is among the common and persistent groundwater pollutants in the United States (*1*). A considerable amount of laboratory research has been devoted to the study of processes that affect the concentration and speciation of chromium in aqueous systems. These processes include reduction of hexavalent chromium (Cr(VI)), the most toxic and mobile oxidation state of chromium, to the less mobile and less toxic Cr(III) by abiotic (*2, 3*) and microbially mediated (*4*−*6*) redox processes, adsorption of Cr(VI) oxyanions on metal oxides (*7*−*9*), microbial biosorption of Cr(VI) (*10*), oxidation of Cr(III) to Cr(VI) by dissolved oxygen (*11*), photoreduction of Cr(VI) (*12*), and precipitation of Cr(III) hydroxides (*13*).

Chromium transport in contaminated groundwater has also been studied extensively (*14*−*16*). However, interpretation of the results of these field studies is confounded by the complexity of Cr(VI) chemistry in natural systems (*17*). Furthermore, uncertainties associated with the magnitudes of ambient groundwater and chemical mass fluxes confound accurate determination of Cr(VI) attenuation rates at affected sites. In principle, contaminant attenuation rates can be characterized more effectively using contaminant mass flux rather than concentration (*18*−*21*). In addition, the ability to directly measure chromium fluxes could be of significant use in predicting the impact of a source zone on down-gradient receptors (*22*) or in quantifying the performance of source zone remediation (*23*−*25*).

Recent field and laboratory tests (*26*−*28*) used a PFM configuration that allowed estimation of the depth-distribution of groundwater and contaminant flux magnitudes but did not provide measures of specific discharge direction. In this paper, we propose a novel configuration of a passive fluxmeter (PFM) capable of providing simultaneous, in situ measures of both the magnitude and the direction of ambient groundwater specific discharge, q_0, and the local ambient subsurface mass flux, J, of a contaminant i. Here, it is assumed J is approximated as the product of concentration, C_i, and specific discharge, q_0, i.e., $J = C_i q_0$; this assumes that advective flux is sufficiently large that diffusive-dispersive flux can be ignored. The new PFM configuration, described here, consists of a permeable cylinder with sections packed with a porous sorbent material having a high sorption capacity for the contaminants of interest and one or more resident tracers.

The interior of the device is divided by permeable walls into four sectors, a center section and three equal-volume outer sectors, as shown in Figure 1. A known quantity of a reversibly sorbed "resident" tracer is uniformly distributed on the sorbent in the center section, while the sorbent in the three outer sectors contains no resident tracer. At time $t = 0$ (Figure 1a), the PFM is inserted into a well located in contaminated aquifer. Horizontal groundwater flow through the device occurs passively due to local hydraulic gradients. Because the groundwater is contaminated, one or more contaminants are intercepted and retained on the PFM sorbent in the up-gradient sectors of the device. At the same time, the groundwater intercepted by the PFM elutes one or more resident tracers from the center sector into the surrounding down-gradient sectors. After a sampling period $t = \Delta t$ (Figure 1b) the PFM is removed from the well. The sorbent material is removed separately from each sector and extracted, and the extract fractions are analyzed to determine the masses of resident tracer and contaminant adsorbed over period $t = \Delta t$. The magnitude and direction of q_0 and J can then be calculated using simple relationships derived from flow and solute transport models (discussed below).

The general method described above could be applied to measurements of J_{Cr}, if the appropriate sorbent and resident tracers were selected. Since Cr(VI) in dilute aqueous solutions at near-neutral pH is present predominately as the oxyanions

* Corresponding author phone: (352)392-9537 ext 1441; fax: (352)-392-3394; e-mail: khatf@ce.ufl.edu.
† Department of Civil & Coastal Engineering, University of Florida.
‡ Department of Environmental Engineering Science, University of Florida.
§ Purdue University.

10.1021/es060268b CCC: $33.50
Published on Web 09/08/2006

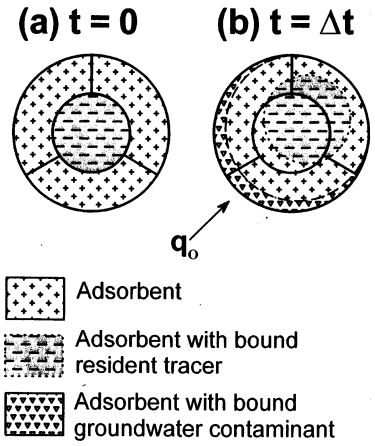

FIGURE 1. Conceptual diagram showing operation of a permeable adsorbent device for simultaneous measurement of groundwater specific discharge and contaminant mass flux. Cross section of the device as deployed in media well (a) and after a deployment period Δt (b).

chromate (CrO_4^{2-}) and bichromate ($HCrO_4^-$), and at higher concentrations as dichromate ($Cr_2O_7^{2-}$) (*29*), an anion exchange resin would seem to be an appropriate choice of sorbent, and any stable anionic compound with the appropriate partitioning behavior could be used as the resident tracer.

The objective of the present study was to evaluate the new PFM configuration using an anion exchange resin as a sorbent and benzoate as the "resident" tracer. Laboratory experiments were designed to assess the accuracy of the PFM for measuring both the magnitude and the direction of ambient specific discharge, q_0, and chromium mass flux, J_{Cr}, in porous media under conditions representing contaminated groundwater flow in an idealized aquifer system. Experimental parameters were selected to reveal the limits of the device's useful range in the measurement of the q_0 and J_{Cr}.

Experimental Section

Chemicals. Stock solutions of benzoic acid, salt, and simulated groundwater buffer (SGB) were prepared according to details provided in the Supporting Information (see page S2).

AG1-X8 anion exchange resin, 20−50 mesh, 1.2 mequiv mL^{-1} capacity, was obtained in the hydroxide form from Bio-Rad Laboratories (Hercules, CA) and was converted to the bicarbonate form by washing slowly with 12 bed volumes of 1 M $NaHCO_3$ and then 12 bed volumes of deionized water. When packed, the AG1-X8(HCO_3^-) resin typically gave a measured bed density (ρ) of 0.7 g cm^{-3} and bed porosity (θ) of 0.63. Because the water content of resin was 39% by weight, inter- and intraporosities of packed resin were respectively estimated at 0.36 and 0.27.

Benzoate resident tracer was loaded onto the resin after the OH^- to HCO_3^- conversion by stirring 10 mL of slurried resin in 50 mL of deionized water and then adding 50 μL of 2 N NaOH and 200 μL of benzoic acid stock solution. After having been stirred for 1 h, the loaded resin was packed into a glass column and washed with 20 bed volumes of deionized water. Assuming that all added benzoate was adsorbed, the maximum adsorbed benzoate concentration obtainable by this procedure was 2.5 mg mL^{-1} of packed wet resin or 3.6 mg/g wet resin; this corresponded to 0.017 mequiv mL^{-1} or 2.3% of packed resin bed capacity. Resin portions with and without loaded tracers were stored slurried in deionized water at room temperature before use.

Cr(VI), Benzoate Isotherms. To each tared 10-mL vial was added a portion of wet, drained AG1-X8 (HCO_3^-) resin weighed to the nearest milligram and 5.0 mL of SGB containing 2 mg mL^{-1} of either Cr(VI) or sodium benzoate. Duplicate control vials contained no resin. All vials were sealed with Teflon-lined septa, placed on a rotary shaker at 30 rpm, and agitated for >40 h in a 20 °C incubator. Aqueous phase concentrations (C_{Aq}, mg mL^{-1}) were determined as described below. Adsorbed masses were calculated from the difference in aqueous mass of solute between vials with and without resin. Adsorbed concentrations (C_{Sorb}, mg g^{-1}) were calculated based on the mass of wet, drained resin. Benzoate linear partitioning coefficient (k_D^B, mL g^{-1}) was calculated from the slope of the benzoate adsorption isotherm.

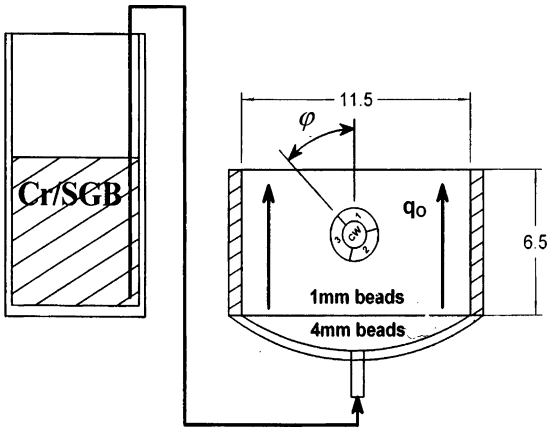

FIGURE 2. Schematic of column setup used to conduct experiments with the permeable adsorbent devices. Column dimensions are given in centimeters. The angle from the vertical is φ.

Media Permeability. The hydraulic conductivities of packed beds of AG1-X8 (HCO_3^-) resin and 1-mm glass beads (K^{resin} and K^{beads}, respectively, cm s^{-1}) were measured using a simple constant head permeameter tube with cross-sectional area $A_{bed} = 2.41$ cm^2 and length $L_{bed} = 10$ cm. Steady flow Q (cm^3 s^{-1}) of SGB was measured at three different constant head differences Δh (cm) using a graduated cylinder and stopwatch, and then hydraulic conductivity was calculated as $K = QL_{bed}/(A_{bed}\Delta h)$ (*30*). For both media the three K measurements had relative standard deviations of <1%. The average of the three measurements was taken as the hydraulic conductivity of the media.

Device Construction. Three passive flux meters (PFMs) with the new configuration were constructed of 50 × 50 mesh milling grade woven wire cloth (McMaster-Carr Supply Company, Atlanta, GA) according to details provided in the Supporting Information (see page S2). These devices possessed nominal dimensions of an outer diameter (D) of 2.4 cm, a center sector diameter (D^{CW}) of 1.2 cm, and a bed length (L) of 2.1 cm. Center sectors averaged 2.33 ± 0.2 cm^3 in volume and contained an initial mass of 5.9 ± 0.2 mg of benzoate after packing with resin preloaded with resident tracer.

Column Experiments. PFMs were tested in columns configured as shown in Figure 2. The PVC columns had an inner diameter (D^{col}) of 11.5 cm and a length (L^{col}) of 6.5 cm. The column cross-sectional area (A^{col}) was 104 cm^2. Columns were packed with 4-mm glass beads (Fisher) to a depth of about 2 cm and then filled to the top with 1-mm glass beads (Supelco). A circle of woven wire cloth was used to separate the two bead layers. This design ensured that the buffer solution fed through the bottom of the column was distributed at an even pressure throughout the bottom section of the column, creating an even upward vertical flow profile throughout the 1-mm bead bed.

After packing, columns were flushed with SGB containing 5 mg L^{-1} Cr(VI) (Cr/SGB). Flow through each column was siphoned via PVC tubing from a reservoir which was

maintained at a constant level by forced feed pumped from a main reservoir. Volumetric feed rates to the constant-level reservoirs were not precisely controlled and ranged from 3 to 10 mL min^{-1}. At time $t = 0$, a PFM prepared as described above was buried in the glass bead bed to a depth of approximately 3 cm from the top edge of the device to the surface of the bed. The PFM was placed in the column with a horizontal axis and with the reference divider between outer sectors 1 and 3 rotated an angle φ, from the vertical. Cr/SGB was then allowed to flow upward through the column, draining from the top of the bed through weir holes cut into the column rim (see Figure 2). The Cr/SGB was collected as it drained from the column, and the collected volume was measured in a graduated cylinder to the nearest 0.1 L. After a volume ΔV (L) had been collected over a sampling period t (h), reflecting a desired specific discharge, flow through the column was stopped and the device removed from the column. The Cr/SGB used in each run was analyzed separately to determine feed Cr(VI) concentration (C^F_{Cr}, mg L^{-1}). A total of 16 runs were conducted in a 4^2 experimental matrix, with the parameters q_θ and ΔV varied over 4 levels each. Experimental values of φ were 0, 45, 90, and 180 degrees, while ΔV levels were 4−5 L, 8−12 L, 19−21 L, and 30−42 L. C^F_{Cr} ranged from 4.8 to 5.7 mg/L for these experiments. The various combinations of applied volumes of Cr/SGB over various sampling periods produced ambient specific discharges q_0, ranging from 0.2 to 0.9 m/d for the Cr/SGB and ambient chromium fluxes J_{Cr}, varying from 1.1 to 5.3 g/m^2/d (see Table S1, Supporting Information). Peclet numbers, calculated according to Hatfield et al. (2004), ranged from 30 to 300 indicating advection dominated transport.

Analytical Methods. After removing the PFM from the column, one end cap was removed from the device, and the resin was scraped out of each sector individually, starting with the center well, using a round-end spatula. Care was taken to remove as much resin as possible from each sector without cross-contaminating resin in adjacent sectors. The resin from each sector was transferred to a 50-mL beaker, slurried in deionized water, then packed into a 1 cm i.d. glass column, and extracted with 20 mL of a resin extraction solution at 0.6 mL min^{-1}. This extraction technique was found to give Cr(VI) and benzoate recoveries of 100 ± 5% (data not shown).

Extract fractions were assayed for Cr(VI) mass (m^{Cr}_i, mg) using the diphenylcarbazide colorimetric method (*31*). Response to Cr(VI) at 540 nm was calibrated using a 3-level standard curve. Benzoate resident tracer mass (m^B_i, mg) in the extract fractions was determined by HPLC using a 25.0 × 0.46 cm Partisil PAC 10 μm column (Alltech Associates, Inc., Deerfield, IL). Mobile phase was 10% (v/v) HPLC-grade acetonitrile (Fisher), 90% 50 mM sodium phosphate pH 3.2, at 1.25 mL min^{-1}. The retention time of benzoic acid by this method was 4.3 min. Samples were diluted a minimum of 1:20 in the mobile phase, and then 0.25 mL was injected. Detection was by UV at 220 nm. Benzoate UV response factor was determined using a 3-level external standard calibration curve. A blank and a calibration check standard were analyzed with each set of samples to verify a stable response.

Results and Discussion

Cr(VI) and benzoate adsorption isotherms at pH 7, 20 °C, are shown in Figure S2 (parts a and b, respectively) in the Supporting Information. Cr(VI) sorption appears to follow a Langmuir isotherm, as expected for the exchange of a divalent anion, such as CrO_4^{2-}, with a monovalent anion, such as HCO_3^- (*32*). Benzoate sorption appears to be linear (r^2 = 0.999), with sorbed concentrations S^B [mg/g] related to dissolved C^B [mg/cm^3] by a linear sorption coefficient (k^B_D, cm^3 g^{-1})

$$S^B = k^B_D C^B \tag{1}$$

The solid line in Figure S2b (Supporting Information) represented (1) with $k^B_D = 288$ cm^3 g^{-1} for benzoate sorption from SGB. It could be that benzoate sorption follows a Langmuir, but that measurements were confined to the linear range.

Benzoate equilibrium sorption on an anion exchange resin would be influenced by the concentrations of competing anions in the aqueous phase. Since column experiments were conducted with buffer reservoirs open to the atmosphere, bicarbonate concentrations could have increased or decreased over time with CO_2 absorption or release. Therefore, it was important to verify that this k^B_D value was valid for each of the 16 column experiments. To verify this, the electrical conductivity of the Cr/SGB feed buffer was monitored for each column experiment and was found to vary by <8% overall runs. Using this k^B_D value with the AG1-X8 bed properties ρ and (θ), a benzoate retardation factor R^B_d was calculated as

$$R^B_d = 1 + \frac{k^B_D \rho}{\theta} = 325 \tag{2}$$

Benzoate tracer results from the 16 PFM experiments for four tested flow directions, φ, are shown in Figure 3. The plot illustrates the relative mass of resident tracer, Ω_R, remaining in the center section of the PFM versus ξ. This latter parameter represents the dimensionless cumulative pore volume of fluid intercepted by the center section over the time period t divided by the retardation factor R^B_d. Thus,

$$\xi = \frac{\alpha q_0 t}{2r\theta R^B_d} \tag{3}$$

in which r is the radius of the center sector (0.006 m), and α is a flow convergence factor (*33*) calculated from the hydraulic conductivities of the resin, K^{resin}, and glass beads, K^{beads}:

$$\alpha = \frac{2K^{resin}}{K^{beads} + K^{resin}} \tag{4}$$

Measured values of K^{resin} and K^{beads} were 0.39 and 0.84 cm s^{-1}, respectively; as a result, $\alpha = 0.64$. It is evident from Figure 3, benzoate is displaced from the center section of the PFM at a rate linearly related to the cumulative volume of water intercepted $\xi \leq 0.5$ or $\Omega_R \geq 0.4$. Furthermore, this elution is independent of flow direction φ.

Under an ambient groundwater flux, q_0, benzoate elution from the center section of the PFM is approximated using one of two models (*26*). The first assumes tracer sorption is linear, reversible, and instantaneous such that

$$\Omega_R = \frac{2}{\pi}[\sin^{-1}(\sqrt{1-\xi^2}) - \xi\sqrt{1-\xi^2}] \tag{5}$$

Included in Figure 3 are predictions from the first model, which produces a linear elution profile with a reciprocal slope equating to R^B_d as $\xi \rightarrow 0$. At the other extreme, the predicted elution profile becomes concave as $\xi \rightarrow 1$ even though the benzoate isotherm is linear. This simulated concavity is a consequence of assuming uniform flow inside the PFM and a uniform initial distribution of resident tracer over the circular center section. This first elution model produces a reasonable comparison to experimental data for values of $\xi \leq 0.5$, and thereafter model predictions diverge from observations. This is equivalent to 1.2 m of cumulative specific

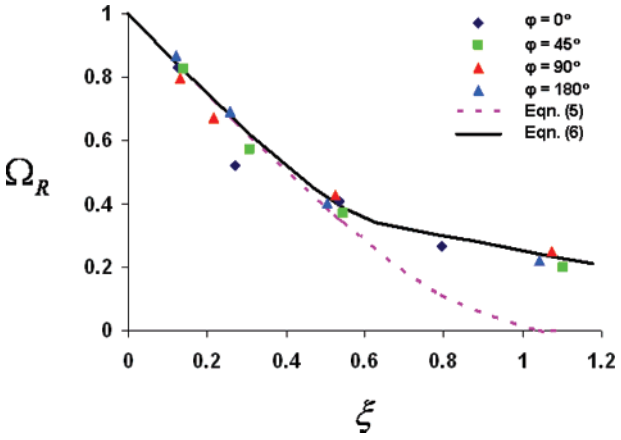

FIGURE 3. Mass fraction of residual benzoate tracer, Ω_R, measured and simulated in each passive flux meter versus the dimensionless pore volumes of water intercepted, ξ.

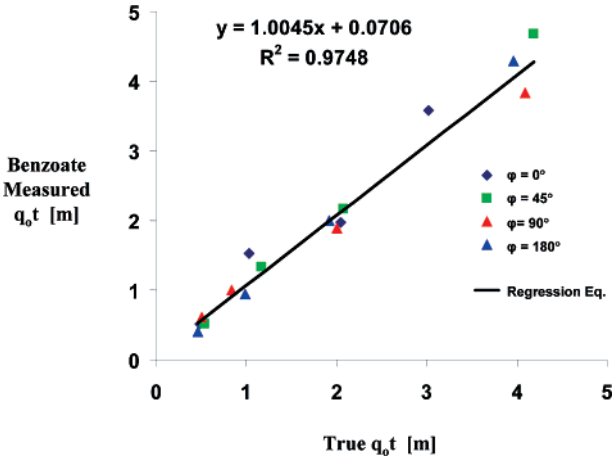

FIGURE 4. Measured cumulative water fluxes $q_0 t$, using the benzoate resident tracer versus true cumulative fluxes in four flow directions φ.

discharge $\alpha q_0 t$, intercepted by the PFM or 1.9 m of ambient cumulative groundwater flux $q_0 t$.

From a practical perspective of interpreting water fluxes using the first model 5, it is preferable that the PFM be retrieved from the aquifer (i.e., well) when $0.25 \leq \xi \leq 0.5$. The lower limit ensures sufficient PFM exposure to ambient conditions for quantifying groundwater fluxes with minimum error (*26*) although Figure 3 displays an excellent comparison between the model and data for values of $\xi \leq 0.25$. Thus, under assumed conditions of an ambient groundwater flux of ~1.0 m/d and $\alpha = 0.64$, optimal PFM retrieval from the aquifer occurs within 1.0 and 1.9 days. For lower ambient groundwater fluxes, a longer exposure period is required to sample within the optimal range of ξ. It is, however, critical that groundwater flux be sufficiently high that advective transport dominates diffusion inside the PFM; thus for $\alpha = 0.64$, the current PFM design is not recommended where the ambient groundwater flux is less than 5.2 cm/d (*26*).

Nonlinear and/or rate-limited tracer desorption can account for differences between predicted and observed benzoate retention for values of $\xi > 0.5$. Nonlinear desorption is not considered plausible here, because desorption experiments (not shown) produce a linear isotherm and a retardation factor comparable to sorption experiments (i.e., $R_d^B = 294$).

Rate-limited tracer elution from PFMs is less efficient and is most evident under elevated flow conditions as ξ increases above 0.5. The last four points to the right side of Figure 3 reflect values of $\xi > 0.5$, generated under the highest specific discharge rates (0.6−0.9 m/d). This is where the first model clearly underestimates the fraction benzoate retained in the center section.

To better capture the apparent tracer retention over the full experimental range of ξ, a second model was tested which simulates elution under conditions of nonlinear and/or rate-limited desorption using a weighted linear combination of independent linear elution terms (*26*)

$$\Omega_R = \frac{2}{\pi}\sum_{i=1}^{P}\eta_i[\sin^{-1}(\sqrt{1-\xi_i^2}) - \xi_i\sqrt{1-\xi_i^2}] \qquad (6)$$

and

$$\xi_i = \frac{\alpha q_0 t}{2r\theta R_{di}^B} \qquad (7)$$

where index i ($i = 1,2,...,p$) is identified as the linear elution function, the applicable retardation factor is R_{di}^B, and the mass fraction of tracer eluted under that function is η_i. Normally, η_i and R_{di}^B would be derived from an experimental tracer elution profiles; however, for this study eq 6 was limited to two terms ($p = 2$) where the mass fraction of tracer eluted under each was assumed the same ($\eta_1 = \eta_2 = 0.5$). Given these limitations, the second model represented the next level of complication beyond eq 5.

Parameters R_{d1}^B and R_{d2}^B are defined as follows using eq 21 in ref *26*

$$R_{d1}^B = \psi R_d^B = 203 \quad R_{d2}^B = \frac{\eta_2 R_d^B}{\left(1 - \frac{\eta_1}{\psi}\right)} = 812 \qquad (8)$$

where ψ is an approximation of the fraction of resident tracer eluted from a streamtube after ψR_d^B pore volumes of flow produce a change in the slope of the elution profile. ψ can be as low as 0.57 (a reflection of mobile water porosity and tracer associated with this porosity) or as high as 0.68 (the linear limit of eq 5). For this study, ψ is conveniently equated to 0.63, the average. The second model [eq 6] is also included in Figure 3, where it appears to better characterize benzoate elution over a suite of 16 experiments. Like the first model, the second produces a predicted elution profile with a reciprocal slope equal to R_d^B as $\xi \rightarrow 0$. The current PFM design has not been studied beyond the maximum tested value of $\xi = 1.2$. Given previous assumed conditions of an ambient groundwater flux of ~1.0 m/d and $\alpha = 0.64$, the current PFM design needs to be retrieved within 4.6 days.

Figure 4 provides a comparison of measured versus true cumulative water flux $q_0 t$ based on the second model and the relative residual mass of benzoate tracer recovered from the sampled center sections of each PFM experiment. The average cumulative water flux prediction error is on the order of −8% with a standard deviation of ±15%.

An equation for calculating flux direction, φ, can be derived from a simple center of mass analogy in which the mass of tracer extracted from each sector of the PFM, m_i ($i = 1,2,3$), is treated as a point mass located at the geometric center of the sector; details are provided in the Supporting Information (see page S4). Using this reference system the direction of water flux (and for that matter contaminant flux) is given by

$$\varphi = -\tan^{-1}\left[\frac{0.866(m_1^B - m_3^B)}{0.5(m_1^B + m_3^B) - m_2^B}\right] \qquad (9)$$

where the coefficients 0.866 and 0.5 correspond to the cosine and sine of 30°, which are the x and y coordinates of the center points of sectors 1 and 3. Note that eq 9 does not

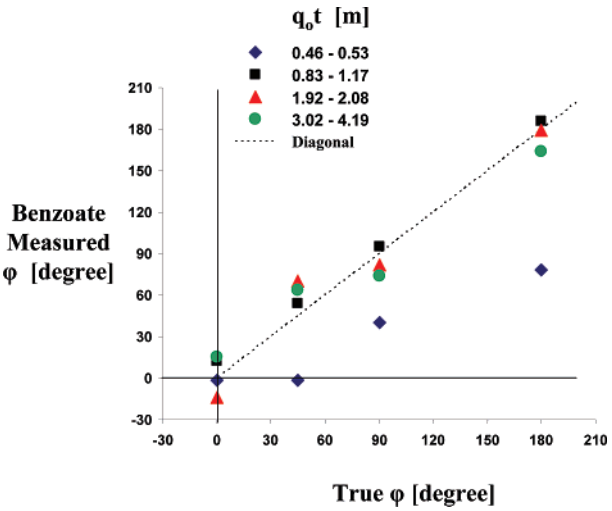

FIGURE 5. Angular component of specific discharge vector φ, measured values from eq 9 versus experimental values for the 16 runs. Dashed line is diagonal for reference.

include the mass of benzoate in the center well, and it applies as shown when $(m_1^B + m_3^B)/2 \geq m_2^B$; otherwise 180 degrees is added to φ from eq 9. Listed in Table S1 of the Supporting Information are benzoate and Cr(VI) data from 16 experiments.

Figure 5 depicts predicted values of φ using eq 9 from the 16 sets of m_i^B data in Table S1 (Supporting Information). Measured φ values are plotted against true angle of flow. For 12 experiments involving cumulative ambient discharges $q_0t \geq 0.83$ m (corresponding to $\Delta V \geq 8.3$ L, $\alpha q_0 t \geq 0.53$ m, and $\xi \geq 0.22$), the average residual error of measured φ was 3° with a standard deviation of ±14°.

Four experiments were conducted under a cumulative ambient groundwater discharge of $q_0t \leq 0.53$ m (corresponding to $\Delta V \leq 5.3$ L, $\alpha q_0 t \leq 0.34$ m, and $\xi < 0.14$), which gave an average residual error of measured φ of 50° with a standard deviation of ±41° degrees. Thus, obtaining accurate measures of φ required PFM exposures long enough to ensure $\xi \geq 0.22$. This would correspond to a duration greater than 0.83 days assuming the current PFM design, an ambient groundwater flux of ~1.0 m/d, and $\alpha = 0.64$. From Table S1 (Supporting Information), it may be observed that benzoate was detected in all three outer sectors in every experiment, including those sectors that were up-gradient of the center well. A possible explanation for this observation is that cross contamination occurred when the center section was packed with resin pre-equilibrated with benzoate.

Cumulative Cr(VI) fluxes $J_{Cr}t$, were calculated from total mass of Cr(VI) extracted from each sector of the PFM using the following equation from ref *26*

$$J_{Cr}t = \frac{1.67 m_{Cr}}{\alpha \pi L} \quad (10)$$

where m_{Cr} is the total mass of Cr(VI) extracted from each sector of the PFM. Figure 6 shows measured cumulative flux $J_{Cr}t$, calculated from the extracted Cr(VI) masses in Table S1 (Supporting Information) using eq 10 plotted against experimental values. Good agreement between measured and experimental values was observed over the 16 runs, giving an average residual error of −12% with a standard deviation of ±23%; thus, the accuracy of measured chromium fluxes was not a function PFM exposure (i.e., for $0.14 \leq \xi \leq 1.2$). Although Cr(VI) was detected in each outer sector extract from every run, no Cr(VI) was detected in the center section for any of the runs (data not shown). This observation shows that Cr(VI) breakthrough was not occurring from up-gradient

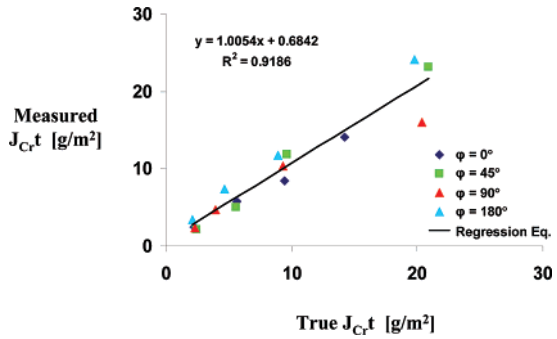

FIGURE 6. Measured cumulative Cr(VI) fluxes $J_{Cr}t$, versus true cumulative fluxes in four flow directions φ.

sectors. The good quantitative Cr(VI) recovery combined with observed lack of breakthrough into the center sector demonstrates that any Cr(VI) transported into the device was effectively bound by the adsorbent. Using an equation analogous to eq 9 to calculate φ from extracted Cr(VI) masses gave poor agreement with experimental φ values (results not shown). This is because Cr(VI) accumulates over the entire outer edge of the adsorbent bed, such that small quantitative errors introduced during adsorbent removal, extraction, and analysis translates to large errors in φ using eq 9. However, it is reasonable to assume that the direction of chromium flux is equal to that of water when advective Cr(VI) transport dominates. An example where this would not be the case is when the device is located in a slow flow field and dispersive transport dominates advection.

Results of laboratory experiments demonstrate the potential utility of PFMs to provide simultaneous measurements of both the magnitude and the direction of ambient groundwater specific discharge (q_0), and Cr(VI) mass flux (J_{Cr}) in contaminated aquifers, and more generally for monitoring transport and attenuation of various groundwater contaminants. Experiments reflect results obtained under advection dominated transport conditions where ambient specific discharges range from 0.2 to 0.9 m/d, chromium concentrations vary from 4.8 to 5.7 mg/L, and ambient chromium fluxes range from 1.1 to 5.3 g/m²/d. The dimensionless parameter ξ represents the cumulative pore volume of fluid intercepted by the center section of the PFM normalized to the tracer retardation factor R_d^B and is shown to be the single most important parameter defining PFM operation and performance. The PFM is demonstrated to be effective at measuring the magnitude and direction of water and contaminant fluxes if $0.25 \leq \xi \leq 1.2$. This corresponds to a PFM sampling duration of 1.0−4.6 days under an ambient groundwater flux of ~1.0 m/d. It is important to emphasize this optimal range for ξ does not change with variations in the PFM radius. However, increasing the diameter of the PFM increases the allowable range groundwater velocities and sampling periods for PFM measurements.

Modification of the PFM design and of the procedures described in this paper could possibly improve the accuracy of the technique. Increasing the sorptive characteristics of the outer sections could minimize the likelihood that tracers are released in the environment. Using multiple resident tracers with a broad range of sorption coefficients k_D could provide redundant measures of both water flux and flow direction over a wider range of groundwater flow rates. For long-term sampling, or when conditions reflect high groundwater fluxes and high ionic strength groundwater, resident tracers with high k_D would be required. However, for short-term sampling durations or opposing conditions of low groundwater fluxes and low groundwater ionic strength, the use of highly mobile resident tracers would be preferable. Clearly, additional laboratory experiments would be needed

to test the current and any new PFM configuration in box aquifers equipped with screened wells. These tests could evaluate the PFM for sensitivity to groundwater quality and transient changes in groundwater flux.

Further study is also needed to test the accuracy and practicality of this new PFM configuration in actual field conditions. Theory assumes a purely horizontal and unidirectional flow field across a PFM. In reality, vertical flow exists, and when a PFM is emplaced over a long period of time, seasonal changes in groundwater level and flow direction induce resident tracer elution in multiple directions. Segmenting PFMs along the vertical axis with impermeable septa or placing multiple PFMs in a well appears to minimize vertical flow in the well (*27*, *28*). However, long-term flux monitoring may be problematic, if natural changes in the horizontal flow direction are not considered when interpreting field results. Finally, a combination of both laboratory and field studies may be needed to resolve concerns that competitive sorption or rate-limited sorption may undermine the ability of the PFM to capture and retain target contaminants.

Acknowledgments

This research was partially funded by the U.S. Department of Defense (project number ER0114) under the Environmental Security Technology Compliance Program (ESTCP), the U.S. Department of Energy (DE-FG02-97ER62471) under Natural and Accelerated Bioremediation Research (NABIR) program, and the Florida Water Resources Research Center under a grant from the U.S. Department of Interior (01HqGR0138)

Supporting Information Available

Details on stock solutions of benzoic acid, salt, and simulated groundwater buffer (SGB), specifics on the construction of the PFM including design and dimensions of PFMs and photograph of an empty device (Figure S1), Cr(VI) and benzoate adsorption isotherms at pH 7, 20 °C (Figure S2), additional information on the derivation of directional eq 9 (text and Figure S3), and benzoate and Cr(VI) data from 16 experiments (Table S1). This material is available free of charge via the Internet at http://pubs.acs.org.

Literature Cited

(1) National Research Council. *Environmental Epidemiology, Vol. 1, Public Health and Hazardous Wastes*; National Academy Press: Washington, DC, 1991; p 108.
(2) Deng, B.; Stone, A. T. Surface-Catalyzed Chromium(VI) Reduction: Reactivity Comparisons of Different Organic Reductants and Different Oxide Surfaces. *Environ. Sci. Technol.* **1996**, *30*, 2484−94.
(3) Kozuh, N.; Stupar, J.; Gorenc, B. Reduction and Oxidation Processes of Chromium in Soils. *Environ. Sci. Technol.* **2000**, *34*, 112−119.
(4) Chen, J. M.; Hao, O. J. Microbial chromium (VI) reduction. *Crit. Rev. Environ. Sci. Technol.* **1998**, *28*, 219−251.
(5) Lovley, D. R. Bioremediation of organic and metal contaminants with dissimilatory metal reduction. *J. Ind. Microbiol.* **1995**, *14*, 85−93.
(6) Shen, H.; Pritchard, P. H.; Sewell, G. W. Microbial Reduction of Cr(VI) during Anaerobic Degradation of Benzoate. *Environ. Sci. Technol.* **1996**, *30*, 1667−1674.
(7) Mikami, N.; Sasaki, M.; Kikuchi, T.; Yasunaga, T. Kinetics of adsorption-deorption of chromate on gamma-AL203 surfaces using the pressure-jump technique. *J. Phys. Chem.* **1983**, *87*, 5245−5248.
(8) Ainsworth, C. C.; Girvin, D. C.; Zachara, J. M.; Smith, S. C. Chromate adsorption on goethite-effects of aluminum substitution. *Soil Sci. Soc. Am. J.* **1989**, *53*, 411−418.
(9) Zachara, J. M.; Girvin, D. C.; Schmidt, R. L.; Resch, C. T. Chromate adsorption on amorphous iron oxyhydroxide in the presence of major groundwater ions. *Environ. Sci. Technol.* **1987**, *21*, 589−594.
(10) Sag, Y.; Atacoglu, I.; Kutsal, T. Simultaneous biosorption of chromium(VI) and copper(II) on Rhizopus arrhizus in packed column reactor: Application of the competitive Freundlich model. *Sep. Sci. Technol.* **1999**, *34*, 3155−3171.
(11) Schroeder, D. C.; Lee, G. F. Potential transformations of chromium in natural-waters. *Water, Air, Soil Pollut.* **1975**, *4*, 355−365.
(12) Hug, S. H.; Laubscher, H. U.; James, B. R. Iron(III) Catalyzed Photochemical Reduction of Chromium(VI) by Oxalate and Citrate in Aqueous Solutions. *Environ. Sci. Technol.* **1997**, *31*, 160−170.
(13) Baes, C. F.; Mesmer, R. E. *The hydrolysis of cations;* Wiley-Interscience: New York, 1976.
(14) Loyaux-Lawniczak, S.; Lecomte, P.; Ehrhardt, J.-J. Behavior of Hexavalent Chromium in a Polluted Groundwater: Redox Processes and Immobilization in Soil. *Environ. Sci. Technol.* **2001**, *35*, 1350−57.
(15) Henderson, T. Geochemical reduction of hexavalent chromium in the Trinity sand aquifer. *Ground Water* **1994**, *32*, 477−486.
(16) Puls, R. W.; Clark, D. A.; Paul, C. J.; Vardy, J. Transport and transformation of hexavalent chromium through soils and into ground water. *J. Soil Contam.* **1994**, *3*, 203−224.
(17) James, B. R. The challenge of remediating chromium-contaminated soil. *Environ. Sci. Technol.* **1996**, *30*, 248A−251A.
(18) API. *Estimating Mass Flux for Decision-Making: An Expert Workshop*; American Petroleum Institute: Washington, DC, 2002.
(19) ITRC. *Assessing the performance of DNAPL source reduction remedies*; Dense Nonaqueous Phase Liquids Team, InterstateTechnology & Regulatory Council: Washington, DC, 2003.
(20) EPA. *The DNAPL Remediation Challenge: Is There a Case for Source Depletion? Expert Panel on DNAPL Remediation*; Kavanaugh, M. C., Rao, P. S. C., Eds.; EPA/600/R-03/143; National Risk Management Research Laboratory, Office of Research and Development, U.S. Environmental Protection Agency: Cincinnati, OH, 2004.
(21) NRC. *Contaminants in the subsurface: Source zone assessment and remediation*; National Academic Press: Washington, DC, 2004.
(22) Einarson, M. D.; McKay, D. M. Predicting impacts of groundwater contamination. *Environ. Sci. Technol.* **2001**, *35*, 66A−73A.
(23) Rao, P. S. C.; Jawitz, J. J.; Enfield, C. G.; Falta, R. W. J.; Annable, M. D.; Wood, A. L.; Technology Integration for contaminated site remediation: clean-up goals and performance criteria. In *Groundwater Quality 2001, Third International Conference on Groundwater Quality*; Thorton, S., Oswald, S., Eds.; University of Sheffield: United Kingdom, 2002; pp 571−578.
(24) Falta, R. W.; Rao, P. S. C.; Basu, N. Assessing the Impacts of Partial Mass Depletion in DNAPL Source Zones: I. Analytical Modeling of Source Strength Functions and Plume Response. *J. Contam. Hydrol.* **2005a**, *78*, 259−280.
(25) Falta, R. W.; Basu, N.; Rao, P. S. C. Assessing Impacts of Partial Mass Depletion in DNAPL Source Zones: II. Coupling Source Strength Functions to Plume Evolution. *J. Contam. Hydrol.* **2005b**, *79*, 45−66.
(26) Hatfield, K.; Annable, M.; Cho, J.; Rao, P. S. C.; Klammler, H. A direct passive method for measuring water and contaminant fluxes in porous media. *J. Contam. Hydrol.* **2004**, *75*, 155−181.
(27) Annable, M. D.; Hatfield, K.; Cho, J.; Klammler, H.; Parker, B.; Cherry, J.; Rao, P. S. C. Field-scale evaluation of the passive flux meter for simultaneous measurment of groundwater and contaminant fluxes. *Environ. Sci. Technol.* **2005**, *39(18)*, 7194−7201.
(28) Basu, N.; Rao, P. S. C.; Poyer, I. C.; Annable, M. D.; Hatfield, K. Flux-based assessment at a manufacturing site contaminate with trichloroethylene. *J. Contam Hydrol.* **2006**, in press.
(29) Stumm, W.; Morgan, J. J. *Aquatic Chemistry;* John Wiley & Sons: New York, 1996.
(30) Bear, J. *Dynamics of Fluids in Porous Media;* American Elsevier Publishing Co.: New York, 1972.
(31) Bartlett, R.; James, B. R. Behavior of chromium in soils. 3. oxidation. *J. Environ. Qual.* **1979**, *8*, 31−35.
(32) Smith, R. P.; Woodburn, E. T. Prediction of multicomponent ion-exchange equilibria for ternary-systems SO^{-2}-(4)-NO^{-}-(3)-CL From data of binary systems. *AIChE J.* **1978**, *24*, 577−587.
(33) Strack, O. D. L. *Groundwater Mechanics*; Prentice Hall: Englewood Cliffs, NJ, 1979.

Received for review February 7, 2006. Revised manuscript received July 22, 2006. Accepted July 31, 2006.

ES060268B